Supporting Information:

High Hole-Mobility Molecular Layer Made from Strong Electron Acceptor Molecules with Metal Adatoms

Hiroyuki Yamane *[†,‡] and Nobuhiro Kosugi [†,‡]

[†] Institute for Molecular Science, National Institutes of Natural Sciences, Myodaiji, Okazaki 444-8585, Japan
[‡] SOKENDAI (The Graduate University for Advanced Studies), Myodaiji, Okazaki 444-8585, Japan
*Corresponding Author: yamane@spring8.or.jp
(Present Address) H.Y.: RIKEN SPring-8 Center, Sayo, Hyogo 679-5148, Japan

In this Supporting Information, we show the extra supporting data for the electronic structure of the F_4TCNQ-Au/Au(111) system studied by angle-resolved photoemission spectroscopy (ARPES) using synchrotron radiation.

A. Surface core-level shift in Au $4f_{7/2}$ photoemission

Figure S1 shows the Au $4f_{7/2}$ photoemission spectra for TCNQ/Au(111) and F_4TCNQ/Au(111). The asymmetric Au $4f_{7/2}$ photoemission lineshape for TCNQ/Au(111) involves a well-known surface core-level shift, where the Au $4f_{7/2}$ of bulk Au and surface Au atoms exist at the binding energy (E_b) of 83.99 eV (labeled B) and 83.75 eV (labeled S), respectively. On the other hand, the Au $4f_{7/2}$ photoemission lineshape for F_4TCNQ/Au(111) is slightly broader than that for TCNQ/Au(111). In order to reproduce the Au $4f_{7/2}$ photoemission lineshape for F_4TCNQ/Au(111), an additional peak at E_b = 83.54 eV (labeled A) is requited, which might be ascribed to the segregated Au adatom.

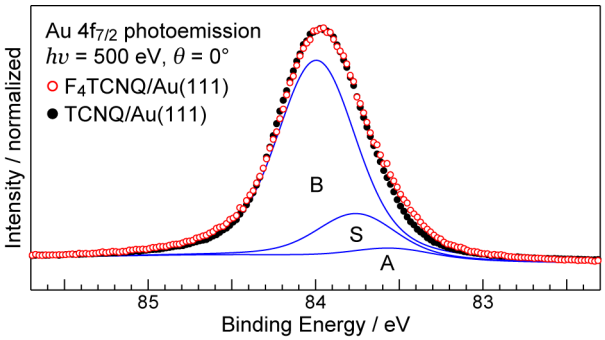

Figure S1. Au $4f_{7/2}$ photoemission spectra for TCNQ/Au(111) and F_4TCNQ/Au(111) at 20 K, together with the fitting curves using Voigt function (solid curve).

B. Temperature dependence of ARPES

Figure S2 shows the ARPES spectra at the emission angle (θ) of 30~42° measured for the clean Au(111) surface at 300 K and the F_4TCNQ/Au(111) interface at 300 K and 20 K. No significant electronic states exist just below the Fermi level (E_F) at the clean Au(111). Upon formation of F_4TCNQ/Au(111) at 300 K, the dispersive electronic states CT_1 and CT_2 are formed just below E_F. The other adsorption-induced peak at E_b = 2.6 eV also shows the dispersion. These dispersive peaks are getting sharpened at 20 K, while the bandwidth is almost unchanged. The broad F 2p peak does not show the dispersion, indicating less contribution to the CT interaction.

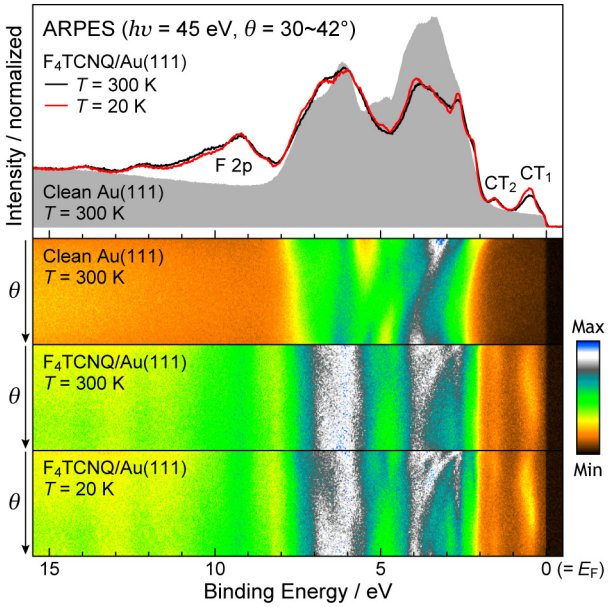

Figure S2. ARPES spectra at θ = 30~42° measured for the clean Au(111) surface at 300 K and the F_4TCNQ monolayer on Au(111) at 300 K and 20 K. The color contour map shows the energy-vs-angle photoemission intensity distribution.

C. Azimuthal-angle dependence of ARPES

Figure S3 shows the azimuthal-angle dependence of the E-$\boldsymbol{k}_{\parallel}$ map for the F_4TCNQ/Au(111) interface at 20 K. Along the $\bar{\Gamma}$-$\bar{K}$ [S3(a)] and $\bar{\Gamma}$-$\bar{M}$ [S3(b)] directions, the CT_1 band exhibits a single component dispersion. On the other hand, along the 10°-off [S3(c)] and 20°-off [S3(d)] directions with respect to the $\bar{\Gamma}$-$\bar{M}$ direction, the CT_1 band exhibits at least two components due to the E-$\boldsymbol{k}_{\parallel}$ measurement for the inequivalent surface Brillouin zone regions [see Figure 4(b) in the main paper].

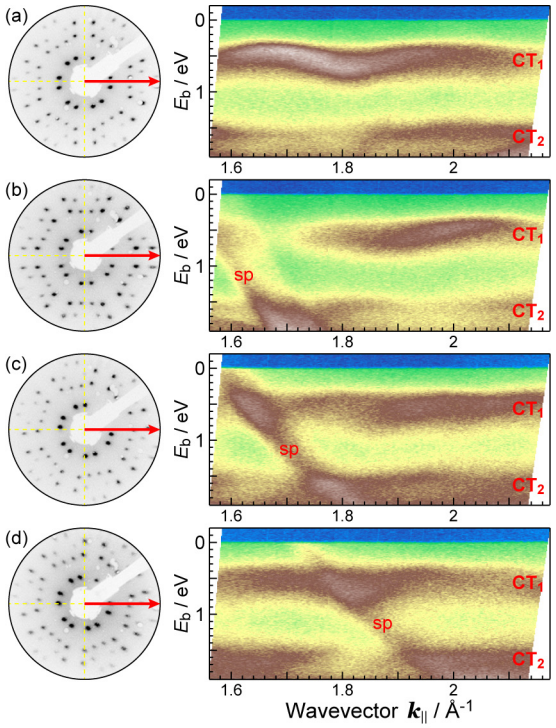

Figure S3. Valence-band dispersion at the F_4TCNQ/Au(111) interface along (a) $\bar{\Gamma}$-$\bar{K}$, (b) $\bar{\Gamma}$-$\bar{M}$, (c) 10°-off $\bar{\Gamma}$-$\bar{M}$, and (d) 20°-off $\bar{\Gamma}$-$\bar{M}$ directions. The corresponding LEED image is given in the left, where the red arrow indicates the scanned direction in the E-$\boldsymbol{k}_{\parallel}$ measurement.

D. Free-electron-like parabolic fitting to CT_1 band

The hole effective mass (m_h^*) is proportional to the inverse of the band curvature, $m_h^* = \hbar^2\left[\mathrm{d}^2E(\boldsymbol{k}_\parallel)/\mathrm{d}\boldsymbol{k}_\parallel^2\right]^{-1}$. The band curvature was determined from the free-electron-like parabolic fitting to the experimental data at $\boldsymbol{k}_\parallel = 0.00\pm0.08$ Å^{-1}, where the peak position (opened circles in Figure S4) is determined from the energy distribution curves. The parabolic fitting, shown by red curve in Figure S4, gives $m_h^* = 0.45m_0$ and $E_b = 0.443$ eV for the CT_1-band dispersion at $\boldsymbol{k}_\parallel = 0$ Å^{-1} ($\bar{\Gamma}$ point).

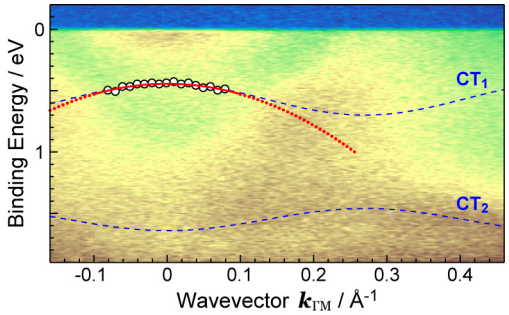

Figure S4. Free-electron-like parabolic fitting to the CT_1 band at F_4TCNQ/Au(111) along the $\bar{\Gamma}$-$\bar{M}$ direction.

E. Thermal desorption experiments using ARPES

Figure S5 shows the normal-emission ARPES spectra for F_4TCNQ/Au(111) and TCNQ/Au(111) as a function of the annealing temperature. The F_4TCNQ multilayer shows the CT-derived peak even at the 50-Å film thickness due to the formation of the extended space charge region.[1] After annealing the F_4TCNQ multilayer at 380 K for 5 min., the CT-derived peaks are getting sharpened and the multilayer components disappears due to the multilayer desorption. The subsequent annealing at 390 K for 5 min. introduces the appearance of the Shockley state (labeled S) due to the partial desorption of the monolayer. On the other hand, the ARPES spectrum of the TCNQ multilayer with the 50-Å film thickness is almost similar to that of the bulk TCNQ.[2] After annealing the TCNQ multilayer at 373 K for 5 min., the Shockley state (S) is getting visible and the multilayer components disappears due to the multilayer desorption. The subsequent annealing at 390 K for 5 min. introduces the broadening of the Shockley state due to the coexistence of the Shockley states at the clean Au(111) surface and at the TCNQ/Au(111) interface by the partial monolayer desorption.

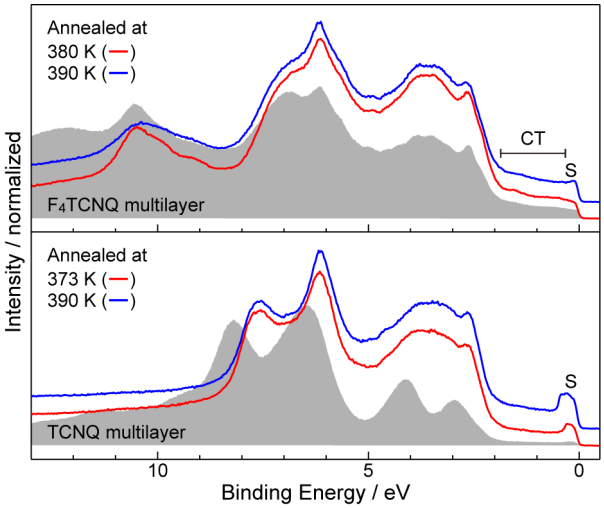

Figure S5. Annealing-temperature-dependent ARPES spectra at $\theta = 0\pm7°$ for F_4TCNQ/Au(111) and TCNQ/Au(111).

References

(1) Gerbert, D.; Maass, F.; Tegeder, P. Extended Space Charge Region and Unoccupied Molecular Band Formation in Epitaxial Tetrafluoro-Tetracyanoquinodimethane Films. *J. Phys. Chem. C* **2017**, *121*, 15696–15701.

(2) Capitán, M. J.; Navío, C.; Beltrán, J. I.; Otero, R.; Álvarez, J. TCNQ Grown on Cu(001): Its Atomic and Electronic Structure Determination. *J. Phys. Chem. C* **2016**, *120*, 26889–26898.